ACS SENSORS

pubs.acs.org/acssensors

Article

Innovative FO-SPR Label-free Strategy for Detecting Anti-RBD Antibodies in COVID-19 Patient Serum and Whole Blood

Jia-Huan Qu, Karen Leirs, Wim Maes, Maya Imbrechts, Nico Callewaert, Katrien Lagrou, Nick Geukens, Jeroen Lammertyn,* and Dragana Spasic

Cite This: https://doi.org/10.1021/acssensors.1c02215

Read Online

ACCESS | Metrics & More | Article Recommendations | Supporting Information

ABSTRACT: The ongoing COVID-19 pandemic has emphasized the urgent need for rapid, accurate, and large-scale diagnostic tools. Next to this, the significance of serological tests (i.e., detection of SARS-CoV-2 antibodies) also became apparent for studying patients' immune status and past viral infection. In this work, we present a novel approach for not only measuring antibody levels but also profiling of binding kinetics of the complete polyclonal antibody response against the receptor binding domain (RBD) of SARS-CoV-2 spike protein, an aspect not possible to achieve with traditional serological tests. This fiber optic surface plasmon resonance (FO-SPR)-based label-free method was successfully accomplished in COVID-19 patient serum and, for the first time, directly in undiluted whole blood, omitting the need for any sample preparation. Notably, this bioassay (1) was on par with FO-SPR sandwich bioassays (traditionally regarded as more sensitive) in distinguishing COVID-19 from control samples, irrespective of the type of sample matrix, and (2) had a significantly shorter time-to-result of only 30 min compared to >1 or 4 h for the FO-SPR sandwich bioassay and the conventional ELISA, respectively. Finally, the label-free approach revealed that no direct correlation was present between antibody levels and their kinetic profiling in different COVID-19 patients, as another evidence to support previous hypothesis that antibody-binding kinetics against the antigen in patient blood might play a role in the COVID-19 severity. Taking all this into account, the presented work positions the FO-SPR technology at the forefront of other COVID-19 serological tests, with a huge potential toward other applications in need for quantification and kinetic profiling of antibodies.

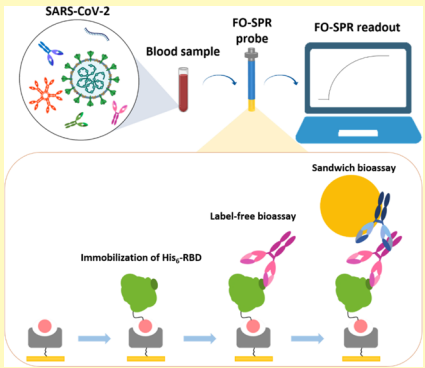

KEYWORDS: *SARS-CoV-2, serological test, FO-SPR, ELISA, His_6-tagged RBD, binding kinetics, serum, whole blood*

Despite the enormous growth of the biosensor field over the past 20 years,[1,2] the ongoing pandemic of coronavirus disease 2019 (COVID-19) has revealed numerous shortcomings of the current biosensors to deliver rapid diagnostic solutions. However, this pandemic has also pointed to the crucial role of biosensing technologies for measuring antibody responses in patients with previous exposure to severe acute respiratory syndrome coronavirus 2 (SARS-CoV-2). In addition to evaluating individual and potential community seroprevalence, these so-called serological tests have been proven useful in supporting many other relevant studies, including (1) selection of convalescent plasma donors for COVID-19 therapy, (2) determining the efficacy of newly developed vaccines, (3) further understanding of the immune responses related to protection, and (4) potentially guiding public health interventions.[3,4]

With the global consensus that serological tests play an important role in controlling and managing the COVID-19 pandemic, a plethora of serological test kits have been developed over the past 2 years, such as enzyme-linked immunosorbent assay (ELISA), chemiluminescent immunoassay, and rapid tests.[5−10] Despite the fact that some of these have actually reached the market, the majority of the COVID-19 serological tests developed to date offer only partial insight into the patient response by solely focusing on the antibody levels. In this context, surface plasmon resonance (SPR)-based biosensors demonstrate clear advantages compared to other platforms because of their capacity for real-time monitoring and label-free detection, which can reveal the binding kinetics of patient antibodies.[11−13] The latter has been shown in many studies to be likely related to the severity of COVID-19, further emphasizing the significance of knowing this information rather than just the antibody levels.[14−18]

Starting from these clear advantages of SPR technology, we present in this work label-free fiber optic (FO)-SPR serological bioassays that enable the measuring of antibody levels as well as kinetic profiling of the polyclonal anti-SARS-CoV-2

Received: October 18, 2021
Accepted: January 12, 2022

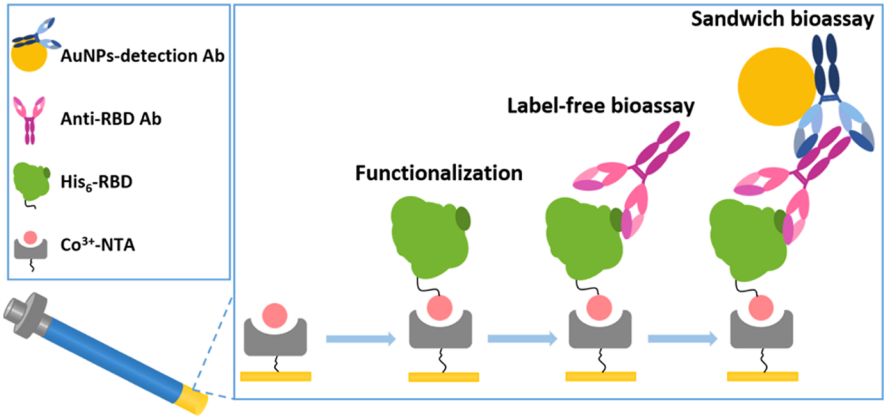

Figure 1. Schematic illustration of the FO-SPR serological bioassays for the detection of anti-SARS-CoV-2 RBD antibodies in label-free and sandwich formats. The His_6-tagged RBD was immobilized on the Au-coated FO probe through Co(III)-NTA surface chemistry for an oriented and stable patterning of the bioreceptor. Depicted detection antibody was either GAH IgG or GAH IgG, IgM, and IgA.

Table 1. Serum and Whole Blood Patient Samples Used for Different Bioassays in This Study (*Blood and Serum Samples Collected from the Same Patients)[a]

	COVID-19 positive/convalescent	COVID-19 negative	bioassays
serum (first series)	P1, P2, P3, P4, P5, P6, P7, P8, P9, P10, P11, P12, P13, P14, P15, P16, P17, P18, P19, P20, P21, P22	N1, N2, N3, N4, N5, N6, N7, N8, N9, N10, N11, N12, N13, N14, N15, HCS	FO-SPR label-free/sandwich in-house ELISA ELISA kit (EuroImmun)
blood*	BP1, BP2, BP3, BP4, BP5, BP6, BP7, BP8, BP9, BP10, BP11, BP12, BP13, BP14	BN1, BN3, BN4, BN5, BN6	FO-SPR label-free/sandwich
serum* (second series)	SP1, SP2, SP3, SP4, SP5, SP6, SP7, SP8, SP9, SP10, SP11, SP12, SP13, SP14	SN1, SN3, SN4, SN5, SN6	FO-SPR label-free

[a]For the first series of serum samples, P and N stand for positive and negative, respectively; for the blood samples, BP and BN stand for blood positive and negative, respectively; for the second series of serum samples, SP and SN stand for serum positive and negative, respectively.

antibody response in COVID-19 patient samples. In this context, the main benefit of the FO-SPR technology is its compatibility with complex matrices,[19−27] thereby allowing inspection of both antibody levels and their kinetic profiling directly in complex matrices (and hence in patient samples), an aspect difficult to attain with conventional chip-SPR configurations because of the potential clogging of microfluidic channels. Therefore, here we establish the FO-SPR bioassays not only in serum but also for the first time directly in the whole blood of convalescent patients (Figure 1). To accomplish this, the His_6-tagged receptor binding domain (RBD) of the SARS-CoV-2 viral spike protein is used as the bioreceptor on the FO probe, immobilized with Co(III)-NTA (stands for cobalt(III)-nitrilotriacetic acid) chemistry. This surface chemistry has been selected to achieve an oriented and stable patterning of the bioreceptors, essential for target detection in complex sample matrices.[22] To evaluate the sensitivity of label-free bioassays in serum and whole blood, we also developed FO-SPR sandwich bioassays, traditionally known as more sensitive bioassays. These are established by using two types of detection antibodies: (1) goat anti-human (GAH) IgG or (2) GAH IgG, IgM, and IgA antibody, conjugated with gold nanoparticles (AuNPs) to enhance the sensitivity of these bioassays. The GAH IgG, IgM, and IgA antibody is included to increase the likelihood of detecting different antibody isotypes in patient samples (rather than just focusing on IgG as reported in the majority of serological bioassays), thus resembling the label-free bioassay.[28,29] The FO-SPR sandwich bioassays are benchmarked with an in-house developed ELISA (using exactly the same bioassay components as on the FO-SPR biosensor) and a commercial ELISA kit (EuroImmun) in a series of COVID-19 convalescent patient samples. Compared to the more frequently reported sandwich bioassays in the context of COVID-19 serological studies, our FO-SPR label-free bioassay offers at least four apparent advantages: (1) information about kinetic binding profiles of antibody responses (not attainable with sandwich bioassays), (2) insight into the complete patient antibody response, (3) shorter time-to-result (i.e., 30 min) compared to sandwich bioassays (e.g., 4 h for a conventional ELISA), and (4) exceptional compatibility with whole blood samples, omitting the need for any sample processing. These innovative aspects, combined with other previously demonstrated FO-SPR attributes, like the low-cost sensor probes, ease of operation, low-demand in sample volume, and even flexibility to integrate with microfluidic platform toward a point-of-care (POC) test,[20−26] position the FO-SPR technology at the forefront of other (rapid) COVID-19 serological tests published to date. Moreover, because our FO-SPR technology has been proven as a highly adaptable platform for detecting >10 different targets,[20−25,30−35] the same approach is easily amenable to other applications in need for testing the levels and kinetic profiling of antibodies.

2. EXPERIMENTAL SECTION

2.1. Reagents and Buffers. Recombinant SARS-CoV-2 spike RBD protein with His-tag (Cat. 40592-V08H) and monoclonal anti-RBD antibody (chimeric: constant domains of human IgG1 with mouse variable regions) (Cat. 40150-D004) were purchased from Sino Biological (Beijing, China). GAH IgG (heavy chain specific) antibody (Cat. 31118) and GAH IgG, IgM, and IgA antibody (heavy and light chains specific) against IgG, IgM, and IgA (Cat. 31128) were purchased from Thermo Fisher Scientific (Massachusetts,

https://doi.org/10.1021/acssensors.1c02215
ACS Sens. XXXX, XXX, XXX−XXX

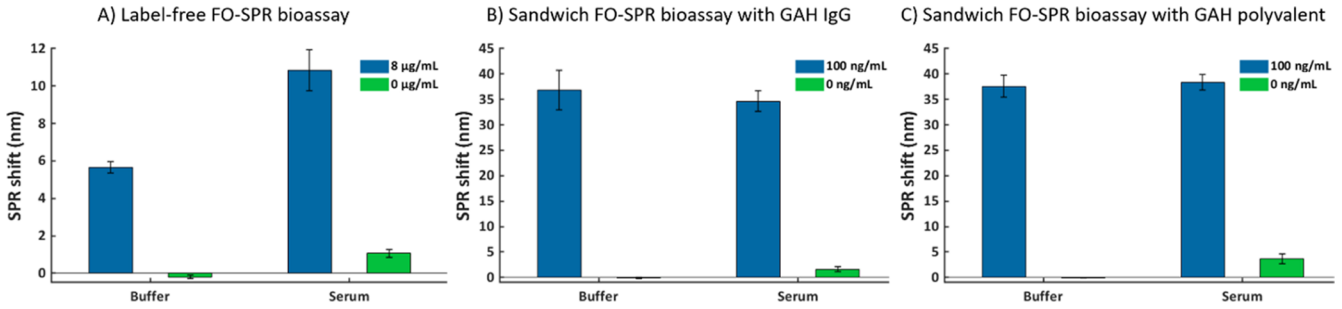

Figure 2. Detection of commercial anti-RBD IgG antibody: (A) at 0 and 8 μg/mL in buffer or 10-fold diluted HCS using the label-free bioassay and (B,C) at 0 and 100 ng/mL in buffer or 500-fold diluted HCS in a sandwich bioassay, using AuNPs functionalized with (B) GAH IgG or (C) GAH IgG, IgM, and IgA antibody. The FO probe was functionalized with 5 μg/mL of RBD for all experiments. Error bars represent 1 SD (n_s = 3).

United States). Anti-IgG GAH (Fc specific) conjugated with horseradish peroxidase (HRP) (A0170) was purchased from Sigma (Missouri, United States). The healthy control serum (HCS), that is, pooled serum samples from healthy controls (HS1044P), was purchased from Valley Biomedical (Winchester, United States). The details about all chemical reagents and buffers used for FO-SPR based label-free and sandwich bioassays can be found in our previous publication[22] and also in the Supporting Information 1.1.

2.2. Patient Samples. As summarized in Table 1, 22 serum samples were obtained from SARS-CoV-2 infected patients (PCR positive) residing in the COVID-19 wards or ICU at the AZ Groeninge hospital in Kortrijk (March−June 2020) (referred to as P1−P22, COVID-19 positive/convalescent in Table 1). Fifteen serum samples, serving as the negative control (NC) in our study, were collected prior to the COVID-19 pandemic (referred to as N1−N15, COVID-19 negative in Table 1). Peripheral blood was collected in BD Vacutainer SST II Advance tubes (Becton, Dickinson and Company, USA) and used to prepare serum that was stored at −20 °C until further use. The study protocol (S64089) was approved by the Ethical Committees (EC) of the University Hospitals of Leuven and AZ Groeninge Hospital (Commissie Medische Ethiek) in Kortrijk.

Fourteen blood samples were collected from COVID-19 convalescent patients (different from the above-mentioned patients for collecting serum samples, referred to as BP1−BP14 in Table 1) who were diagnosed with COVID-19 (i.e., PCR positive) between March 2020 and March 2021 (i.e., with a range of 2−14 months between COVID-19 diagnosis and sampling). Additionally, five blood samples from healthy donors not previously diagnosed with COVID-19 were obtained and served as the NC (referred to as BN1, BN3, BN4, BN5, and BN6 in Table 1). The blood samples were collected in 6 mL BD Vacutainer glass citrate tubes containing 3.2% sodium citrate as the anti-coagulant (Becton, Dickinson and Company, USA) and stored at 4 °C for performing FO-SPR bioassays within 1 week. These blood samples were also further processed for preparing matching serum samples (referred to as SP1−SP14 (COVID-19 convalescent) and SN1, SN3, SN4, SN5, and SN6 (COVID-19 negative) in Table 1) by collecting blood in BD Vacutainer SST II Advance tubes (Becton, Dickinson and Company, USA). The study protocol (S65369) was approved by the EC (i.e., Ethics Commission Research UZ/KU Leuven).

2.3. FO-SPR label-free and sandwich bioassay in serum and whole blood. The FO-SPR biosensor (FOx Biosystems, Diepenbeek, Belgium) used to perform all bioassays in this work was commercialized based on our in-house developed FO-SPR biosensor prototype[20] as described in Figure S1A and our previous work.[22−24] The gold-coated FO sensor probe was manufactured as elaborated before[21,36] and then further functionalized with His_6-tagged RBD as the bioreceptor. The details are described in Supporting Information 1.2 and Figure S1B following our previously developed Co(III)-NTA-based bioassays.[22]

In the label-free bioassays, the functionalized FO probes were immersed for 30 min in different solutions depending on the type of analysis: (1) the detection buffer (PBST: 10 mM PBS pH 7.4 with 0.01% Tween 20) spiked with the target (i.e., commercial anti-RBD IgG antibody), (2) serum/whole blood from COVID-19 negative samples (diluted with the detection buffer) spiked with the same target, or (3) serum/whole blood both from COVID-19 convalescent patients and COVID-19 negative samples, diluted with the detection buffer. In the sandwich bioassays, the signal amplification was performed after the label-free step, with the FO probes immersed in AuNPs (optical density, OD = 1.0), functionalized with GAH IgG or GAH IgG, IgM, and IgA antibody, for 30 min, as described in the previously developed sandwich bioassays.[22−24] Specifically, the serum or whole blood samples were diluted 10-fold for label-free bioassays and 500-fold for sandwich bioassays as will be further elaborated in the following sections.

2.4. Validation of FO-SPR Sandwich Bioassay by ELISA. The home-made ELISA was developed in the Laboratory for Therapeutic and Diagnostic Antibodies (KU Leuven, Belgium). Whereas the details can be found in Supporting Information 1.3, in brief, serum samples (minimally 500-fold diluted) and monoclonal anti-RBD antibody were added to plates coated with His_6-tagged RBD. After 2 h of incubation, the GAH IgG HRP conjugate was incubated for 1 h, followed by addition of the *o*-phenylenediamine dihydrochloride substrate. After 30 min, the reaction was stopped with H_2SO_4 (4 M), and absorbance was measured at 492 nm. A commercial anti-SARS-CoV-2 ELISA (Product no. 2606-10, EuroImmun, Lübeck, Germany) for detection of anti-Spike IgG antibodies was performed following the manufacturer's instructions.[37]

2.5. Data Analysis. FO-SPR data were collected by FOx software (FOx Biosystems) and further analyzed in Matlab 2019b (The MathWorks Inc., Natick). The detection signals (i.e., SPR shift within the 30 min of association phase) were processed for both label-free and sandwich bioassays. SPR slopes within the first 120 s of the association phase of the label-free binding steps were also extracted by linear regression. The cutoff value was calculated by summing the average and 3 times the standard deviation (SD) of the NC.[38,39] For the correlation of SPR shift in label-free and sandwich bioassays, the correlation between the obtained SPR shift and slope from the same label-free bioassay, or the correlation between the concentration quantified by the in-house developed ELISA and the commercial kit, the signals were first normalized by dividing each value with the mean of all values for all samples, which could reduce the effect of overlap.[40] To quantify the correlation between the label-free and sandwich bioassays in detecting the total pool of anti-RBD antibodies, Pearson correlation coefficients (PCCs) and intraclass correlation coefficients (ICCs) were calculated in Matlab. For the ICC analysis, the level of reliability was defined based on the ICC values, which were interpreted as poor (<0.5), moderate (0.5−0.75), good (0.75−0.9), and excellent (>0.9).[41] One-way analysis of variance and Bonferroni multiple comparison tests were performed in Matlab to identify the statistical differences between the mean values (α = 0.05).[42]

3. RESULTS AND DISCUSSION

3.1. Anti-RBD antibody detection in spiked buffer and serum samples using FO-SPR bioassays. To establish

https://doi.org/10.1021/acssensors.1c02215
ACS Sens. XXXX, XXX, XXX−XXX

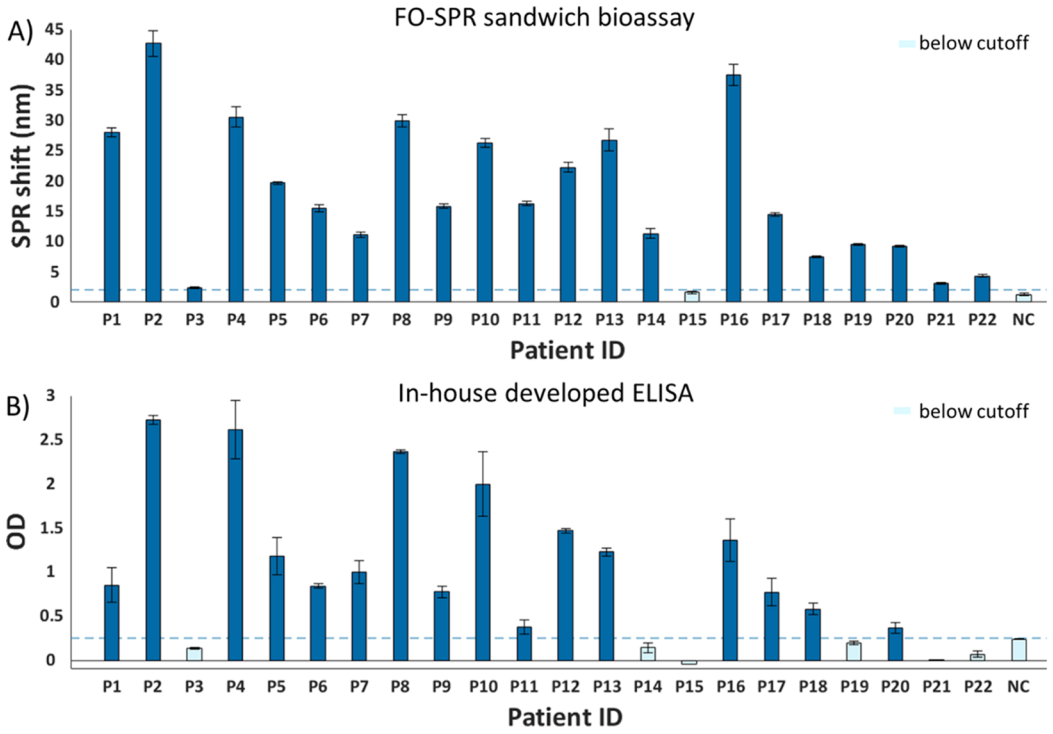

Figure 3. Obtained signals for the detection of IgG antibodies against RBD in 500-fold diluted COVID-19 patient serum samples and HCS as the NC using the (A) FO-SPR sandwich bioassay and (B) in-house developed ELISA. The cutoff value was calculated by summing the average and 3 times SD of the NC. Error bars represent 1 SD (A: n_s = 3; B: n_s = 2).

the FO-SPR bioassays for detection of anti-RBD antibodies, we used His_6-tagged RBD on the FO probe as the bioreceptor and commercial anti-RBD IgG antibody as the target spiked in both buffer and serum. Initially, we tested different concentrations of His_6-tagged RBD for the functionalization of the FO probe. Because the NTA-coated surface was saturated in 30 min when applying at least 5 μg/mL of His_6-tagged RBD (Figure S2), this concentration was used throughout the study.

Next, to select a suitable serum sample as the NC, we tested 15 serum samples from different patients and 1 commercial HCS, which were all obtained before the COVID-19 pandemic (i.e., February 2017 to February 2020). These samples were diluted 500-fold (to match the best performing dilution for ELISA) and tested by introducing AuNPs functionalized with the GAH IgG antibody but without any spiked anti-RBD antibodies. Although the nonspecific signals from the 15 samples varied from 0.4 to 3.4 nm in SPR shifts (which was probably due to the slight changes in the serum composition and amplified by the functionalized AuNPs used in the sandwich bioassay), their average was comparable to the obtained background signal from the HCS (Figure S3). This allowed us to use the HCS as the single NC throughout the paper as well as the matrix to spike the anti-RBD IgG antibody in the following experiments.

To establish the label-free bioassays, we spiked 8 μg/mL of the commercial anti-RBD IgG antibody in both buffer and 10-fold diluted HCS (Figure 2A). This concentration of 8 μg/mL was selected based on our previously reported dynamic range for the FO-SPR label-free bioassay.[22] The HCS and buffer without the spiked antibody (0 μg/mL) were used as the NC. While this NC showed a minimal to nonexistent shift in buffer, the signal was slightly higher in diluted HCS. This is possibly due to the nonspecific interaction of serum components with the FO probe surface and/or the presence of the antibodies against similar antigens (e.g., originating from seasonal coronavirus strains) in the HCS that have cross-reactivity with SARS-CoV-2 RBD, which might also explain why the overall signal in serum is higher than that in the buffer. Nevertheless, spiking the anti-RBD IgG antibody in either buffer or 10-fold diluted HCS demonstrated significantly higher SPR shifts compared to the NCs, pointing to highly specific detection. It is important to mention that 10-fold dilution of HCS was selected among the other tested serum dilutions (undiluted, 20-, 50-, and 100-fold) because it showed the best performance taking into account both specific and nonspecific signals, while allowing minimal dilution of the sample (Figure S4).

Next, we also built the sandwich FO-SPR bioassays using AuNPs for signal amplification, functionalized with GAH IgG or GAH IgG, IgM, and IgA detection antibody (Figure 2B,C, respectively). Here, we spiked 100 ng/mL of anti-RBD IgG antibody in both buffer and 500-fold diluted HCS, while the corresponding matrix without spiked antibodies was used as the NC. Similar to the label-free bioassays, the NC signal was slightly higher in diluted HCS than in the buffer but overall about 20-fold (Figure 2B) or 10-fold (Figure 2C) lower compared to the signal obtained from the spiked samples. Interestingly, a comparable signal was obtained with the two differently functionalized AuNPs in both buffer and diluted HCS, revealing their equivalent ability in binding IgG antibodies. In conclusion, our established FO-SPR label-free and sandwich bioassays were proven suitable for specific detection of anti-RBD antibodies in serum and hence were used for testing patient serum samples as described further.

3.2. Benchmarking FO-SPR Sandwich Bioassay with ELISA. Before testing 22 COVID-19 patient serum samples with the FO-SPR label-free approach, we first analyzed them

https://doi.org/10.1021/acssensors.1c02215
ACS Sens. XXXX, XXX, XXX−XXX

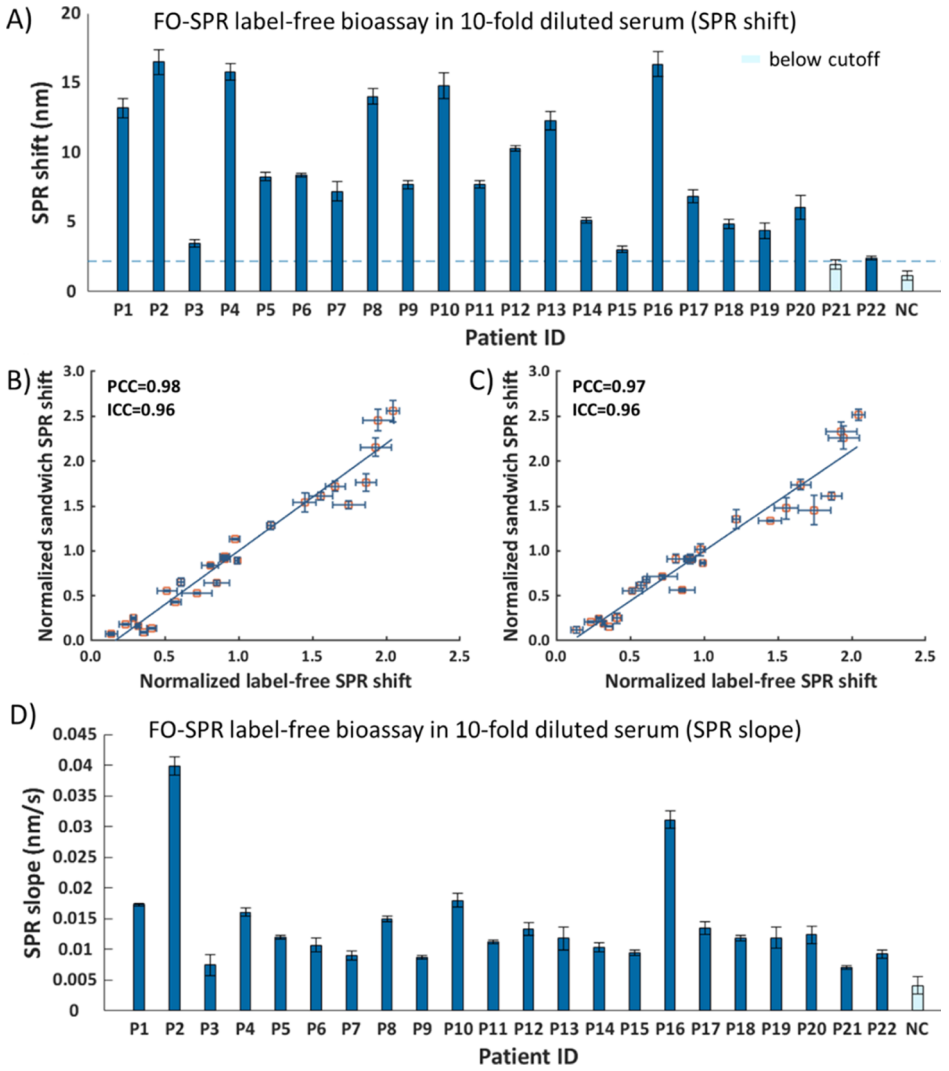

Figure 4. (A) Obtained SPR shift for label-free detection of anti-RBD antibodies in 10-fold diluted COVID-19 patient serum samples and HCS as the NC. The cutoff value was calculated by summing the average and 3 times SD of the NC. (B,C) Correlation between the obtained SPR shift from label-free and sandwich detection using AuNPs functionalized with (B) GAH IgG and (C) GAH IgG, IgM, and IgA antibody. COVID-19 patient serum samples were 10-fold (label-free) and 500-fold (sandwich) diluted. (D) Obtained SPR slopes from the same label-free detection of anti-RBD antibodies in 10-fold diluted COVID-19 patient serum samples and HCS as the NC. Error bars represent 1 SD (n_s = 3).

using more conventional sandwich bioassays. Here, AuNPs functionalized with the GAH IgG antibody were used to specifically target anti-RBD IgG antibodies for the signal amplification in 500-fold diluted serum samples. As revealed by Figure 3A, the tested samples showed a broad variety of the obtained SPR shifts, reflecting different antibody levels. In order to determine which of these samples can be differentiated from the 500-fold diluted HCS (serving as NC), we calculated the cutoff value based on the NC (for details, see Section 2.5 and summary in Table S1). Out of the 22 tested patient samples, only 1 sample (P15) was below the cutoff value. Although we generated the calibration curves for both label-free and sandwich bioassays by spiking the anti-RBD IgG antibody in the buffer (Figure S5), when analyzing patient samples we focused only on the raw signals obtained from the antibody binding (i.e., SPR shifts) rather than their concentrations, similar to majority of the published work related to COVID-19 serological tests.[5−10] This was done for two reasons: (1) these calibration curves are established using a single antibody and as such cannot represent different isotypes of antibodies generated in response to a virus that also differ in quantity and ratios among different patients[43−45] and (2) knowing the exact concentration of antibodies in COVID-19 patients has not yet been proven as valuable information and requires further investigation from different research disciplines, including clinicians, immunologists, and so forth.

To evaluate the performance of the established FO-SPR-based sandwich bioassay and benchmark this technology, we also tested the same patient serum samples (500-fold dilution) using an in-house developed ELISA. This ELISA was built by using the same bioassay components as on the FO-SPR platform and by adapting a previously published ELISA protocol toward the detection of anti-RBD IgG antibodies.[46] As depicted in Figure 3B, using the ELISA, six samples (P3, P14, P15, P19, P21, and P22) could not be discriminated from the HCS (serving as NC) based on the cutoff value. Moreover, when compared to FO-SPR, few additional samples (e.g., P1, P9, P11, and P13) revealed the overall underestimation of antibody levels by ELISA, which was probably due to the long incubation steps leading to the dissociation of antibodies with

https://doi.org/10.1021/acssensors.1c02215
ACS Sens. XXXX, XXX, XXX−XXX

low affinity, thereby causing lower signals.[47] Thanks to the FO-SPR real-time monitoring of binding events, no dissociation of bound antibodies from the FO-SPR surface was observed during the short washing step for 3 min. Therefore, we can conclude that the FO-SPR sandwich bioassay had substantially better performance compared to ELISA in distinguishing the COVID-19 positive samples from the NC. Moreover, the FO-SPR data variability (CV = 4.7 ± 3%, n_s = 3) was much smaller than that from ELISA (CV = 13 ± 12.5%, n_s = 2), demonstrating a higher reproducibility using FO-SPR. It is important to mention that we also compared this in-house developed ELISA with a commercial ELISA kit (EuroImmun). As shown in Figure S6A, the level of anti-RBD antibodies measured by the in-house ELISA (Figure S6B) showed a good correlation (PCC = 0.85, ICC = 0.84) with the titer of anti-S1 IgG antibodies measured by the commercial assay (Figure S6C), similar to previous reports.[48−50]

3.3. FO-SPR Label-Free Bioassay for Measuring the Antibody Levels and Profiling of Binding Kinetics in Patient Serum Samples. As described in Section 3.1, detection of the commercial anti-RBD IgG antibody using the FO-SPR label-free bioassay was proven feasible in both buffer and 10-fold diluted serum. Therefore, the same 22 COVID-19 patient serum samples, tested with the FO-SPR sandwich bioassay and ELISA, were further assessed in a label-free manner (Figure 4A). All samples were diluted 10-fold, including the HCS used as the NC. Similar to sandwich bioassays, we have applied the cutoff value to evaluate which samples can be distinguished from the NC, with the results summarized in Table S1. Based on this, only one patient sample (P21) was below the cutoff value. Although this patient sample was a different one compared to the sample below the cutoff value in the FO-SPR sandwich bioassay (P15), they both also showed extremely low OD values in ELISA, suggesting that these patients have very low levels of antibodies, difficult to differentiate from the NC. Nevertheless, we can conclude that the performance of the label-free bioassay was largely comparable if not on par with the sandwich bioassay, the latter traditionally known for its superior sensitivity. This was further verified by the excellent correlation (PCC = 0.98, ICC = 0.96) between the label-free and sandwich bioassays (Figure 4B). A similar correlation (PCC = 0.97, ICC = 0.96) was also obtained between FO-SPR label-free and sandwich bioassays performed with GAH IgG, IgM, and IgA antibody, the latter included to resemble label-free detection of all antibody isotypes (IgG, IgM, and IgA) (Figure 4C). Based on the results presented in Figure S7 (i.e., significantly higher level of total antibody pool versus IgG for more than half of the tested patient samples), one might expect that the correlation would have been even better when using GAH IgG, IgM, and IgA antibody. This was however not the case, revealing that IgG remains the predominant isotype in the majority of patients. Nevertheless, we cannot completely rule out that GAH IgG, IgM, and IgA antibody might have different affinity toward different antibody isotypes, which then does not allow to have a true representation of different antibody isotypes in the sample. Contrary to this, a label-free bioassay gives direct insight into the entire antibody pool, being as such of unprecedented value. In this context, it is important to mention that some patient anti-RBD antibodies might form different complexes with other nonspecific antigens or cells from blood samples. Although we cannot completely rule out the interference of these complexes with the performed bioassays, this is also highly unlikely to happen because we acquired highly reproducible label-free and sandwich bioassay data for different tested patient samples, as it can be seen from the provided binding curves (Figure S8), SPR shift, and SPR slope values (Figure 4).

Additionally, we also calculated the SPR slopes from the label-free binding curves (Figure S8) within the first 2 min for all tested COVID-19 patient serum samples (Figure 4D). Next to the level of antibodies, these slope values are known to reflect the binding rate of the target to the bioreceptor immobilized on the FO probe (i.e., antibodies to the RBD, respectively), thereby giving insight into the kinetic profile of patient antibodies. Although determining the avidity of those antibodies is not trivial to achieve, because of the lack of knowledge on their concentration and ratio of different isotypes, the obtained overall profiles are certainly informative. For instance, strong binding curves were observed for both P2 and P16 in Figure S8, with a quickly saturated sensing surface and a high final shift. This probably revealed the existence of a dominant binding antibody with high affinity against the immobilized RBD in addition to a high concentration. Contrary to this, a completely distinctive binding profile was observed for P10 and P13, which might suggest that within the same sample, binding of different antibody types and with different affinities occurs over several phases. Furthermore, by comparing the trends of the SPR shift and slope signals in Figure 4A,D, it is evident that there is no straightforward correlation between the levels of antibodies and their kinetics, which was additionally proven by the poor correlation (PCC = 0.75, ICC = 0.75) between the SPR shift and slope in Figure S9. For instance, the SPR shift obtained from sample P2 was only slightly higher than those of P1 and P4, whereas the SPR slope was more than double compared to the other two. This revealed that not all patient serum samples with a high SPR shift inevitably resulted in a high SPR slope and vice versa, probably due to the difference in the overall avidity of the antibodies against RBD in different patient samples. This reflects the biological diversity in antibody repertoire, affinity maturation status, and class switching between individuals for any specific antigen.

In conclusion, we have demonstrated an outstanding performance of the FO-SPR label-free bioassay, which is partly associated with an extremely low nonspecific signal, even when using only 10-fold diluted serum. This proved yet again the superior performance of the FO-SPR biosensor using Co(III)-NTA chemistry in complex sample matrices, which enabled both oriented and stable immobilization of bioreceptors.[19,22,27,30] Furthermore, the label-free bioassay with time-to-result (TTR) of 30 min was accomplished 2 times faster compared to the FO-SPR sandwich bioassays (TTR: 67 min) or in a fraction of time compared to the in-house made ELISA (TTR: 4 h), thereby offering a rapid alternative to more conventional approaches without compromising on the sensitivity. Most importantly, the label-free bioassay allowed direct insight into the total level of all antibody isotypes, including their kinetic binding profiling with significant value in clinical studies, the aspects not possible to attain with any of the sandwich bioassays.

3.4. Testing Patient Whole Blood Samples with FO-SPR Label-Free and Sandwich Bioassays. In order to further expand the applicability of the developed label-free FO-SPR bioassay, we also tested it using whole blood samples (10-fold diluted) from 14 COVID-19 convalescent patients (Table

https://doi.org/10.1021/acssensors.1c02215
ACS Sens. XXXX, XXX, XXX−XXX

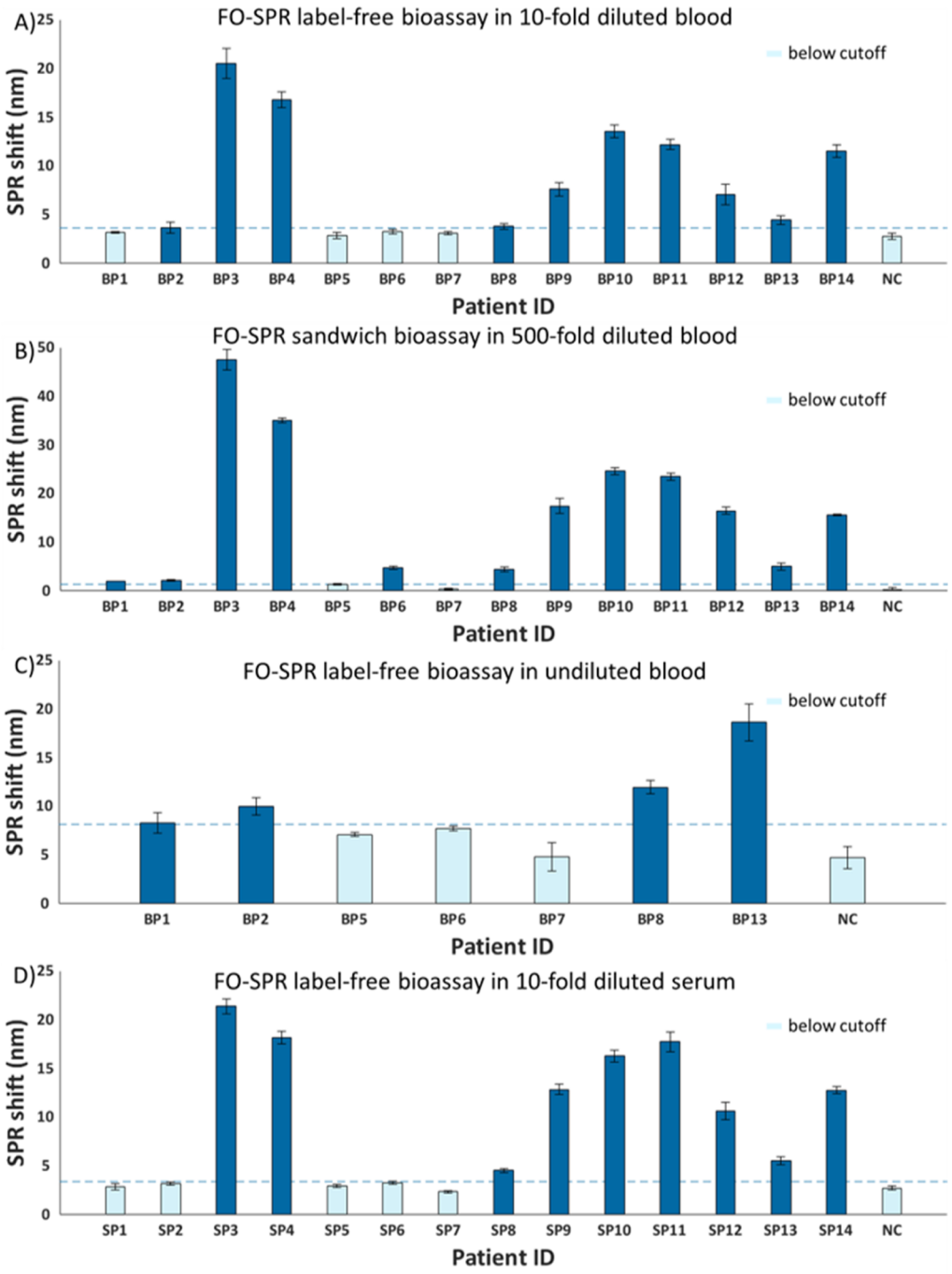

Figure 5. Obtained SPR shifts for the (A) label-free bioassay in 10-fold diluted blood samples, showing the detection of all isotypes of antibodies against RBD, (B) FO-SPR sandwich bioassay in 500-fold diluted blood samples, showing the detection of anti-RBD IgG antibodies, (C) label-free bioassay in undiluted blood samples detecting all isotypes of antibodies against RBD, and (D) label-free bioassay in 10-fold diluted serum samples (second series) detecting all isotypes of antibodies against RBD. The blood and serum samples are from the same donors, with the positive ones from COVID-19 convalescent patients. The cutoff value was calculated by summing the average and 3 times SD of the NC. Error bars represent 1 SD (A: n_s = 3; B: n_s = 3; C: n_s = 2; D: n_s = 3).

1). It is important to note that these samples have been collected from a different set of patients compared to those used for collecting serum samples (indicated as the first series in Table 1). As the NC, we included the equal mixture of five COVID-19 negative blood samples (BN1, BN3, BN4, BN5, BN6), with the respective signals obtained in label-free and sandwich bioassays shown in Figure S10. The same 10-fold diluted NC was also used for spiking 8 μg/mL of the commercial anti-RBD IgG antibody, serving as a positive control to characterize the specificity of the bioassay in blood. The detection of anti-RBD IgG antibody in the diluted blood sample proved to be specific (Figure S11A), allowing us to further test patient samples. As summarized in Table S1 and Figure 5A, four samples (BP1, BP5, BP6, and BP7) were below the cutoff value, which could be explained with the fact that certain blood samples were collected from convalescent patients diagnosed with COVID-19 more than a year ago, thereby resulting in the absence of antibodies (or their

https://doi.org/10.1021/acssensors.1c02215
ACS Sens. XXXX, XXX, XXX−XXX

extremely low levels) against RBD in blood.[51−53] This was further confirmed by identifying the same two samples (BP5, BP7) below cutoff value when performing a sandwich bioassay, traditionally recognized as more sensitive, in 500-fold diluted blood samples (Figure 5B and Table S1). The excellent correlation between label-free and sandwich bioassays in whole blood was further confirmed by both PCC and ICC using AuNPs conjugated with either GAH IgG (PCC = 0.98, ICC = 0.92) or GAH IgG, IgM, and IgA (PCC = 0.98, ICC = 0.92) antibody (Figure S12), further suggesting that the label-free bioassay had highly comparable performance in detecting patient antibodies. It is important to mention here that, similar to the sandwich bioassay in serum, we used again AuNPs functionalized with either GAH IgG or GAH IgG, IgM and IgA antibody, which did not make a difference (Figures S12 and S13), while the specificity of the sandwich bioassay in whole blood was proven by spiking the 500-fold diluted NC with the commercial anti-RBD IgG antibody (Figure S11B).

Next, we wanted to test whether the sensitivity of the label-free bioassay could be additionally improved by using undiluted blood samples. Here, we selected the seven samples with the lowest SPR shift (BP1, BP2, BP5, BP6, BP7, BP8, and BP13) from Figure 5A. As it can be seen from Figure 5C, reducing the dilution factor of blood samples allowed one additional sample (BP1) to be distinguished from the NC based on the cutoff value (Table S1). This has also demonstrated the remarkable feasibility of the FO-SPR platform to deliver highly sensitive label-free bioassays in undiluted blood samples, which could tremendously simplify the sample preparation and be of great significance toward developing true POC biosensors.

Additionally, to investigate if the detecting performance of the FO-SPR technology is dependent on the sample matrix, we performed the label-free bioassay using 14 serum samples (indicated as second series in Table 1) prepared from the same blood samples shown in Figure 5A. The equal mixture of five COVID-19 negative serum samples (SN1, SN3, SN4, SN5, and SN6) was used as the NC. A very similar trend was observed between blood and serum samples, with five serum samples (SP1, SP2, SP5, SP6, and SP7) below the cutoff value (Figure 5D), which was one extra (SP2) compared to the blood test (Figure 5A). This excellent correlation between the label-free bioassays performed in whole blood and serum samples was confirmed by both PCC (0.96) and ICC (0.96) (Figure S14), further demonstrating the independency of the technology on the sample matrix.

Finally, we also looked into the SPR slopes obtained from the label-free bioassay in 10-fold diluted whole blood samples (Figure S15A) as well as their corresponding serum samples (Figure S15B) from 14 COVID-19 convalescent patients using the binding curves. Similar to the binding curves as observed in Figure S8 and elaborated in Section 3.3, the binding profiles were quite different among different patient samples with some showing dominant binding antibodies (e.g., BP3/SP3 and BP4/SP4) and others revealing more binding phases (e.g., BP10/SP10, BP11/SP11, and BP14/SP14). Moreover, comparable to our observations in the previously tested serum samples (Section 3.3), the different trends in the SPR shift and slope signals for the blood (Figure S16A−C) and serum (Figure S16D−F) samples reflected the poor correlation between the levels of antibodies and their kinetics in both matrices. This yet again demonstrated the usefulness of the label-free approach, allowing us to inspect directly the kinetics profile next to the combined levels of all antibody isotypes even in a complex matrix like whole blood.

4. CONCLUSIONS

In this work, we have demonstrated the outstanding capacity of the label-free FO-SPR bioassay to deliver information for both the amount and binding kinetic profiles of antibodies against SARS-CoV-2 RBD. This was established not only in COVID-19 patient serum samples but also for the first time in whole blood.[19] Before testing the patient samples, we successfully developed FO-SPR label-free and sandwich bioassays by spiking a commercial anti-RBD IgG antibody in buffer, serum, and whole blood. His_6-tagged RBD was immobilized as the bioreceptor on the FO probe through Co(III)-NTA surface chemistry to achieve an oriented and stable patterning, which was endurable in complex matrices as we previously reported.[19,22,30] To achieve signal amplification in the sandwich bioassay, we employed AuNPs functionalized with either GAH IgG or GAH IgG, IgM, and IgA antibody, the latter introduced to resemble the label-free bioassay by having the capacity to recognize IgG, IgM, and IgA antibodies.

After characterizing the specificity of the established sandwich FO-SPR bioassay, we further compared it with an ELISA, developed using the same bioassay components and benchmarked with a commercial ELISA kit (EuroImmun). Based on the statistical analysis of 22 COVID-19 patient serum samples (500-fold dilution), the FO-SPR sandwich bioassay showed substantially better performance compared to ELISA in distinguishing the COVID-19 positive samples from the NC. This superior FO-SPR performance was maintained even when testing the same samples (10-fold dilution) using the label-free format while offering a significantly shorter TTR (30 min) compared to the sandwich bioassay (TTR: 67 min) and the in-house developed ELISA (TTR: 4 h). Most importantly, the label-free bioassay also revealed the binding kinetic profiles of polyclonal antibodies against the immobilized RBD, which is not possible to achieve with any of the sandwich bioassays. This additional information provides valuable input for clinical studies as it has been reported that the antibody-binding kinetics against the antigen in patient blood could be associated with the COVID-19 severity.[14−17] Our data further supported these observations by revealing that there was no direct correlation between antibody levels and their kinetics, which reflects the biological diversity in antibody repertoire, affinity maturation status, and class switching between individuals for any specific antigen.

Finally, to further expand the applicability of the developed label-free FO-SPR bioassay in complex matrices, we also tested 14 whole blood samples collected from COVID-19 convalescent patients. Based on the statistical analysis, the FO-SPR label-free bioassay was highly comparable to the sandwich bioassay in its capacity to discriminate the samples from the NC. Interestingly, this was even further improved by performing the label-free bioassays in undiluted blood samples. This not only demonstrated the feasibility of performing the FO-SPR bioassay in a matrix as complex as undiluted whole blood, resulting from the oriented and stable immobilization of His_6-tagged bioreceptors using Co(III)-NTA chemistry, but also pushed the FO-SPR technology one-step further to developing true POC biosensors without the need for sample pretreatment or dilutions. Additionally, we also proved the independency of the FO-SPR technology from the sample matrix by label-free detection of the patient serum samples

https://doi.org/10.1021/acssensors.1c02215
ACS Sens. XXXX, XXX, XXX−XXX

collected from the same donors as the whole blood, which resulted in similar detection. Moreover, we were able to obtain the antibody kinetics profiling in whole blood samples as well, which, similar to the serum samples, revealed poor correlation with the antibody levels.

Overall, we have systematically verified the outstanding capabilities of the label-free FO-SPR bioassays for serological testing of COVID-19 patient serum and whole blood samples, acquiring information about both the level of antibodies and their binding kinetic profiles. Following additional validations with more patient samples, this approach can provide critical added values for other COVID-19 related studies, like selection of convalescent plasma donors for therapy and evaluating the efficacy of developed vaccines. Altogether, the presented work has once again expanded the applications of the FO-SPR biosensing technology with great prospect in the diagnosis or investigation of other diseases.

■ ASSOCIATED CONTENT

Supporting Information

The Supporting Information is available free of charge at https://pubs.acs.org/doi/10.1021/acssensors.1c02215.

Elaborated protocols for FO-SPR bioassays and ELISA; selection of RBD concentrations for immobilization; selection of serum samples as the NC for FO-SPR bioassays; selection of dilution factors for the serum sample in label-free bioassays; calibration curves for the FO-SPR label-free and sandwich bioassays in the buffer; correlation between the in-house developed ELISA and the commercial ELISA kit (EuroImmun); correlation between the obtained SPR shift and slope in label-free detection of patient serum and blood samples; label-free binding curves for testing patient serum and blood samples; detailed data in testing serum and blood samples with two differently functionalized AuNPs; characterization of label-free and sandwich bioassays in blood; profiles of SPR shift (antibody level) and SPR slope (antibody-binding kinetics) in label-free detection of patient blood and serum samples; and table summarizing the performance in testing the patient serum and whole blood samples by cutoff values (PDF)

■ AUTHOR INFORMATION

Corresponding Author

Jeroen Lammertyn − *Department of Biosystems, Biosensors Group, KU Leuven, 3001 Leuven, Belgium;* orcid.org/0000-0001-8143-6794; Email: jeroen.lammertyn@kuleuven.be

Authors

Jia-Huan Qu − *Department of Biosystems, Biosensors Group, KU Leuven, 3001 Leuven, Belgium*

Karen Leirs − *Department of Biosystems, Biosensors Group, KU Leuven, 3001 Leuven, Belgium*

Wim Maes − *PharmAbs, KU Leuven, 3000 Leuven, Belgium*

Maya Imbrechts − *PharmAbs, KU Leuven, 3000 Leuven, Belgium*

Nico Callewaert − *AZ Groeninge Hospital, 8500 Kortrijk, Belgium*

Katrien Lagrou − *Department of Microbiology, Immunology and Transplantation, Laboratory of Clinical Bacteriology and Mycology, KU Leuven, 3000 Leuven, Belgium; Department of Laboratory Medicine and National Reference Centre for Respiratory Pathogens, University Hospitals Leuven, 3000 Leuven, Belgium*

Nick Geukens − *PharmAbs, KU Leuven, 3000 Leuven, Belgium*

Dragana Spasic − *Department of Biosystems, Biosensors Group, KU Leuven, 3001 Leuven, Belgium*

Complete contact information is available at: https://pubs.acs.org/10.1021/acssensors.1c02215

Author Contributions

J.-H.Q. designed the experiments, carried out the FO-SPR related experiments, analyzed and interpreted the data, and wrote the manuscript. K.L.[a] designed the experiments, interpreted the data, supervised the work, and prepared the manuscript. W.M. provided the EuroImmun-related data and critical input and prepared the manuscript; M.I. provided the ELISA-related data and critical input and prepared the manuscript; N.C. provided us with the patient serum samples and prepared the manuscript; K.L.[d,e] was responsible for the application of ethical approval in collecting blood samples from COVID-19 positive and negative volunteers and prepared the manuscript; N.G. provided critical input and prepared the manuscript; J.L. conceived the study, was in charge of the overall direction and planning, interpreted the data, supervised the work, and prepared the manuscript; D.S. conceived the study, designed the experiments, interpreted the data, supervised the work, and wrote the manuscript. All authors provided their critical feedback on the manuscript and gave approval to the final version of the manuscript.

Notes

The authors declare the following competing financial interest(s): Professor Jeroen Lammertyn is a board member of FOx Biosystems, a spin-off company of KU Leuven commercializing FO-SPR technology, next to the principal investigator of the Biosensors group.

■ ACKNOWLEDGMENTS

This work received funding from Research Foundation—Flanders (FWO SBO/S006319N), KU Leuven KOOR (project number ZKD8270), and KU Leuven (project SARS-CoV-2 mAb-OF2).

■ REFERENCES

(1) Chen, C.; Wang, J. Optical Biosensors: An Exhaustive and Comprehensive Review. *Analyst* **2020**, *145*, 1605−1628.

(2) Tu, J.; Torrente-Rodríguez, R. M.; Wang, M.; Gao, W. The Era of Digital Health: A Review of Portable and Wearable Affinity Biosensors. *Adv. Funct. Mater.* **2020**, *30*, 1906713.

(3) Amanat, F.; Stadlbauer, D.; Strohmeier, S.; Nguyen, T. H. O.; Chromikova, V.; McMahon, M.; Jiang, K.; Arunkumar, G. A.; Jurczyszak, D.; Polanco, J.; et al. A Serological Assay to Detect SARS-CoV-2 Seroconversion in Humans. *Nat. Med.* **2020**, *26*, 1033−1036.

(4) Lerner, A. M.; Eisinger, R. W.; Lowy, D. R.; Petersen, L. R.; Humes, R.; Hepburn, M.; Cassetti, M. C. The COVID-19 Serology Studies Workshop: Recommendations and Challenges. *Immunity* **2020**, *53*, 1−5.

(5) GeurtsvanKessel, C. H.; Okba, N. M. A.; Igloi, Z.; Bogers, S.; Embregts, C. W. E.; Laksono, B. M.; Leijten, L.; Rokx, C.; Rijnders, B.; Rahamat-Langendoen, J.; et al. An Evaluation of COVID-19 Serological Assays Informs Future Diagnostics and Exposure Assessment. *Nat. Commun.* **2020**, *11*, 3436.

(6) Kubina, R.; Dziedzic, A. Diagnostics Molecular and Serological Tests for COVID-19. A Comparative Review of SARS-CoV-2

Coronavirus Laboratory and Point-of-Care Diagnostics. *Diagnostics* **2020**, *10*, 434.
(7) Mohit, E.; Rostami, Z.; Vahidi, H. A Comparative Review of Immunoassays for COVID-19 Detection. *Expet Rev. Clin. Immunol.* **2021**, *17*, 573−599.
(8) Ravi, N.; Cortade, D. L.; Ng, E.; Wang, S. X. Diagnostics for SARS-CoV-2 Detection: A Comprehensive Review of the FDA-EUA COVID-19 Testing Landscape. *Biosens. Bioelectron.* **2020**, *165*, 112454.
(9) Serre-Miranda, C.; Nobrega, C.; Roque, S.; Canto-Gomes, J.; Silva, C. S.; Vieira, N.; Barreira-Silva, P.; Alves-Peixoto, P.; Cotter, J.; Reis, A.; et al. Performance Assessment of 11 Commercial Serological Tests for SARS-CoV-2 on Hospitalised COVID-19 Patients. *Int. J. Infect. Dis.* **2021**, *104*, 661−669.
(10) EUA Authorized Serology Test Performance. https://www.fda.gov/medical-devices/coronavirus-disease-2019-covid-19-emergency-use-authorizations-medical-devices/eua-authorized-serology-test-performance (accessed on May 31, 2021).
(11) Djaileb, A.; Charron, B.; Jodaylami, M. H.; Thibault, V.; Coutu, J.; Stevenson, K.; Forest, S.; Live, L. S.; Boudreau, D.; Pelletier, J. N.; et al. A Rapid and Quantitative Serum Test for SARS-CoV-2 Antibodies with Portable Surface Plasmon Resonance Sensing. **2020**, ChemRxiv 10.26434.
(12) Walker, S. N.; Chokkalingam, N.; Reuschel, E. L.; Purwar, M.; Xu, Z.; Gary, E. N.; Kim, K. Y.; Helble, M.; Schultheis, K.; Walters, J.; et al. SARS-CoV-2 Assays To Detect Functional Antibody Responses That Block ACE2 Recognition in Vaccinated Animals and Infected Patients. *J. Clin. Microbiol.* **2020**, *58*, No. e01533.
(13) Huo, J.; Le Bas, A.; Ruza, R. R.; Duyvesteyn, H. M. E.; Mikolajek, H.; Malinauskas, T.; Tan, T. K.; Rijal, P.; Dumoux, M.; Ward, P. N.; et al. Neutralizing Nanobodies Bind SARS-CoV-2 Spike RBD and Block Interaction with ACE2. *Nat. Struct. Mol. Biol.* **2020**, *27*, 846−854.
(14) Yao, X.-Y.; Liu, W.; Li, Z.-Y.; Xiong, H.-L.; Su, Y.-Y.; Li, T.-D.; Zhang, S.-Y.; Zhang, X.-J.; Bi, Z.-F.; Deng, C.-X.; et al. Neutralizing and Binding Antibody Kinetics of COVID-19 Patients during Hospital and Convalescent Phases. **2020**, medRxiv 2020.07.18.20156810.
(15) Wang, Y.; Zhang, L.; Sang, L.; Ye, F.; Ruan, S.; Zhong, B.; Song, T.; Alshukairi, A. N.; Chen, R.; Zhang, Z.; et al. Kinetics of Viral Load and Antibody Response in Relation to COVID-19 Severity. *J. Clin. Invest.* **2020**, *130*, 5235−5244.
(16) Tang, J.; Ravichandran, S.; Lee, Y.; Grubbs, G.; Coyle, E. M.; Klenow, L.; Genser, H.; Golding, H.; Khurana, S. Antibody Affinity Maturation and Plasma IgA Associate with Clinical Outcome in Hospitalized COVID-19 Patients. *Nat. Commun.* **2021**, *12*, 1221.
(17) Ren, L.; Zhang, L.; Chang, D.; Wang, J.; Hu, Y.; Chen, H.; Guo, L.; Wu, C.; Wang, C.; Wang, Y.; et al. The Kinetics of Humoral Response and Its Relationship with the Disease Severity in COVID-19. *Commun. Biol.* **2020**, *3*, 780.
(18) Graham, N. R.; Whitaker, A. N.; Strother, C. A.; Miles, A. K.; Grier, D.; McElvany, B. D.; Bruce, E. A.; Poynter, M. E.; Pierce, K. K.; Kirkpatrick, B. D.; et al. Kinetics and Isotype Assessment of Antibodies Targeting the Spike Protein Receptor-Binding Domain of Severe Acute Respiratory Syndrome-Coronavirus-2 in COVID-19 Patients as a Function of Age, Biological Sex and Disease Severity. *Clin. Transl. Immunol.* **2020**, *9*, No. e1189.
(19) Qu, J. *Developing Innovative FO-SPR Bioassays with Oriented Patterning of Bioreceptors for Diverse Biomedical Applications*; KU Leuven, 2021.
(20) Lu, J.; Van Stappen, T.; Spasic, D.; Delport, F.; Vermeire, S.; Gils, A.; Lammertyn, J. Fiber Optic-SPR Platform for Fast and Sensitive Infliximab Detection in Serum of Inflammatory Bowel Disease Patients. *Biosens. Bioelectron.* **2016**, *79*, 173−179.
(21) Lu, J.; Spasic, D.; Delport, F.; Van Stappen, T.; Detrez, I.; Daems, D.; Vermeire, S.; Gils, A.; Lammertyn, J. Immunoassay for Detection of Infliximab in Whole Blood Using a Fiber-Optic Surface Plasmon Resonance Biosensor. *Anal. Chem.* **2017**, *89*, 3664−3671.
(22) Qu, J.-H.; Horta, S.; Delport, F.; Sillen, M.; Geukens, N.; Sun, D.-W.; Vanhoorelbeke, K.; Declerck, P.; Lammertyn, J.; Spasic, D. Expanding a Portfolio of (FO-) SPR Surface Chemistries with the Co (III)-NTA Oriented Immobilization of His6-Tagged Bioreceptors for Applications in Complex Matrices. *ACS Sensors* **2020**, *5*, 960−969.
(23) Qu, J.-H.; Leirs, K.; Escudero, R.; Strmšek, Ž.; Jerala, R.; Spasic, D.; Lammertyn, J. Novel Regeneration Approach for Creating Reusable FO-SPR Probes with NTA Surface Chemistry. *Nanomaterials* **2021**, *11*, 186.
(24) Yildizhan, Y.; Vajrala, V. S.; Geeurickx, E.; Declerck, C.; Duskunovic, N.; De Sutter, D.; Noppen, S.; Delport, F.; Schols, D.; Swinnen, J. V.; et al. FO-SPR Biosensor Calibrated with Recombinant Extracellular Vesicles Enables Specific and Sensitive Detection Directly in Complex Matrices Journal of Extracellular Vesicles. *J. Extracell. Vesicles* **2021**, *10*, No. e12059.
(25) Qu, J.-H.; Dillen, A.; Saeys, W.; Lammertyn, J.; Spasic, D. Advancements in SPR Biosensing Technology: An Overview of Recent Trends in Smart Layers Design, Multiplexing Concepts, Continuous Monitoring and in Vivo Sensing. *Anal. Chim. Acta* **2020**, *1104*, 10.
(26) Ordutowski, H.; Qu, J.; Verbruggen, R.; Dal Dosso, F.; Safdar, S.; Geukens, N.; Thomas, D.; Spasic, D.; Lammertyn, J. Point-of-Care Solution for Therapeutic Drug Monitoring Enabled By Integrating FO-SPR Readout Into A Self-Powered. *MicroTAS*; Chemical and Biological Microsystems Society, 2020.
(27) Qu, J.-H.; Peeters, B.; Delport, F.; Vanhoorelbeke, K.; Lammertyn, J.; Spasic, D. Gold Nanoparticle Enhanced Multiplexed Biosensing on a Fiber Optic Surface Plasmon Resonance Probe. *Biosens. Bioelectron.* **2021**, *192*, 113549.
(28) Figueiredo-Campos, P.; Blankenhaus, B.; Mota, C.; Gomes, A.; Serrano, M.; Ariotti, S.; Costa, C.; Nunes-Cabaço, H.; Mendes, A. M.; Gaspar, P.; et al. Seroprevalence of Anti-SARS-CoV-2 Antibodies in COVID-19 Patients and Healthy Volunteers up to 6 Months Post Disease Onset. *Eur. J. Immunol.* **2020**, *50*, 2025−2040.
(29) Sanchez, T. W.; Zhang, G.; Li, J.; Dai, L.; Mirshahidi, S.; Wall, N. R.; Yates, C.; Wilson, C.; Montgomery, S.; Zhang, J.-Y.; et al. Immunoseroproteomic Profiling in African American Men with Prostate Cancer: Evidence for an Autoantibody Response to Glycolysis and Plasminogen-Associated Proteins. *Mol. Cell. Proteomics* **2016**, *15*, 3564−3580.
(30) Horta, S.; Qu, J.-H.; Dekimpe, C.; Bonnez, Q.; Vandenbulcke, A.; Tellier, E.; Kaplanski, G.; Delport, F.; Geukens, N.; Lammertyn, J.; et al. Co(III)-NTA Mediated Antigen Immobilization on a Fiber Optic-SPR Biosensor for Detection of Autoantibodies in Autoimmune Diseases: Application in Immune-Mediated Thrombotic Thrombocytopenic Purpura. *Anal. Chem.* **2020**, *92*, 13880−13887.
(31) Daems, D.; Lu, J.; Delport, F.; Mariën, N.; Orbie, L.; Aernouts, B.; Adriaens, I.; Huybrechts, T.; Saeys, W.; Spasic, D.; et al. Competitive Inhibition Assay for the Detection of Progesterone in Dairy Milk Using a Fiber Optic SPR Biosensor. *Anal. Chim. Acta* **2017**, *950*, 1−6.
(32) Knez, K.; Spasic, D.; Delport, F.; Lammertyn, J. Real-Time Ligation Chain Reaction for DNA Quantification and Identification on the FO-SPR. *Biosens. Bioelectron.* **2015**, *67*, 394−399.
(33) Peeters, B.; Safdar, S.; Daems, D.; Goos, P.; Spasic, D.; Lammertyn, J. Solid-Phase PCR-Amplified DNAzyme Activity for Real-Time FO-SPR Detection of the MCR-2 Gene. *Anal. Chem.* **2020**, *92*, 10783.
(34) Daems, D.; Pfeifer, W.; Rutten, I.; Saccà, B.; Spasic, D.; Lammertyn, J. Three-Dimensional DNA Origami as Programmable Anchoring Points for Bioreceptors in Fiber Optic Surface Plasmon Resonance Biosensing. *ACS Appl. Mater. Interfaces* **2018**, *10*, 23539−23547.
(35) Bian, S.; Lu, J.; Delport, F.; Vermeire, S.; Spasic, D.; Lammertyn, J.; Gils, A. Development and Validation of an Optical Biosensor for Rapid Monitoring of Adalimumab in Serum of Patients with Crohn's Disease. *Drug Test. Anal.* **2018**, *10*, 592−596.

https://doi.org/10.1021/acssensors.1c02215
ACS Sens. XXXX, XXX, XXX−XXX

(36) Arghir, I.; Delport, F.; Spasic, D.; Lammertyn, J. Smart Design of Fiber Optic Surfaces for Improved Plasmonic Biosensing. *New Biotechnol.* **2015**, *32*, 473−484.
(37) EuroImmun ELISA kit. https://www.euroimmun.com/products/infection-diagnostics/pd/emerging-diseases/2606/8/96546/ (accessed on March 21, 2021).
(38) Van Stappen, T.; Billiet, T.; Vande Casteele, N.; Compernolle, G.; Brouwers, E.; Vermeire, S.; Gils, A. An Optimized Anti-Infliximab Bridging Enzyme-Linked Immunosorbent Assay for Harmonization of Anti-Infliximab Antibody Titers in Patients with Inflammatory Bowel Diseases. *Inflamm. Bowel Dis.* **2015**, *21*, 2172−2177.
(39) Van den Berghe, N.; Truffot, A.; Peeters, M.; Compernolle, G.; Brouwers, E.; Soenen, R.; Grine, L.; Gils, A.; Imbrechts, M. Development and Validation of Immunoassays for Monitoring of Guselkumab and Anti-Guselkumab Antibodies in Patients with Moderate-to-Severe Psoriasis. *J. Pharm. Biomed. Anal.* **2020**, *189*, 113433.
(40) Wang, Y.; Gao, W.; Noda, I.; Yu, Z. A Modified Mean Normalization Method to Reduce the Effect of Peak Overlap in Two-Dimensional Correlation Spectroscopy. *J. Mol. Struct.* **2006**, *799*, 128−133.
(41) Koo, T. K.; Li, M. Y. A Guideline of Selecting and Reporting Intraclass Correlation Coefficients for Reliability Research. *J. Chiropr. Med.* **2016**, *15*, 155−163.
(42) Borgo, M.; Soranzo, A.; Grassi, M. Data Analysis. *MATLAB for Psychologists*; Springer, 2012; pp 153−187.
(43) Li, L.; Tong, X.; Chen, H.; He, R.; Lv, Q.; Yang, R.; Zhao, L.; Wang, J.; Xu, H.; Liu, C.; et al. Characteristics and Serological Patterns of COVID-19 Convalescent Plasma Donors: Optimal Donors and Timing of Donation. *Transfusion* **2020**, *60*, 1765−1772.
(44) Schasfoort, R. B. M.; van Weperen, J.; van Amsterdam, M.; Parisot, J.; Hendriks, J.; Koerselman, M.; Karperien, M.; Mentink, A.; Bennink, M.; Krabbe, H.; et al. Presence and Strength of Binding of IgM, IgG and IgA Antibodies against SARS-CoV-2 during CoViD-19 Infection. *Biosens. Bioelectron.* **2021**, *183*, 113165.
(45) Peterhoff, D.; Glück, V.; Vogel, M.; Schuster, P.; Schütz, A.; Neubert, P.; Albert, V.; Frisch, S.; Kiessling, M.; Pervan, P.; et al. A Highly Specific and Sensitive Serological Assay Detects SARS-CoV-2 Antibody Levels in COVID-19 Patients That Correlate with Neutralization. *Infection* **2021**, *49*, 75−82.
(46) Bian, S.; Stappen, T. V.; Baert, F.; Compernolle, G.; Brouwers, E.; Tops, S.; Vries, A. d.; Rispens, T.; Lammertyn, J.; Vermeire, S.; et al. Generation and Characterization of a Unique Panel of Anti-Adalimumab Specific Antibodies and Their Application in Therapeutic Drug Monitoring Assays. *J. Pharm. Biomed. Anal.* **2016**, *125*, 62−67.
(47) Beeg, M.; Burti, C.; Allocati, E.; Ciafardini, C.; Banzi, R.; Nobili, A.; Caprioli, F.; Garattini, S.; Gobbi, M. Surface Plasmon Resonance Unveils Important Pitfalls of Enzyme-Linked Immunoassay for the Detection of Anti-Infliximab Antibodies in Patients' Sera. *Sci. Rep.* **2021**, *11*, 14976.
(48) Isho, B.; Abe, K. T.; Zuo, M.; Jamal, A. J.; Rathod, B.; Wang, J. H.; Li, Z.; Chao, G.; Rojas, O. L.; Bang, Y. M.; et al. Persistence of Serum and Saliva Antibody Responses to SARS-CoV-2 Spike Antigens in COVID-19 Patients. *Sci. Immunol.* **2020**, *5*, No. eabe5511.
(49) Salazar, E.; Kuchipudi, S. V.; Christensen, P. A.; Eagar, T.; Yi, X.; Zhao, P.; Jin, Z.; Long, S. W.; Olsen, R. J.; Chen, J.; et al. Convalescent Plasma Anti-SARS-CoV-2 Spike Protein Ectodomain and Receptor-Binding Domain IgG Correlate with Virus Neutralization. *J. Clin. Invest.* **2020**, *130*, 6728−6738.
(50) Yamayoshi, S.; Yasuhara, A.; Ito, M.; Akasaka, O.; Nakamura, M.; Nakachi, I.; Koga, M.; Mitamura, K.; Yagi, K.; Maeda, K.; et al. Antibody Titers against SARS-CoV-2 Decline, but Do Not Disappear for Several Months. *EClinicalMedicine* **2021**, *32*, 100734.
(51) Long, Q.-X.; Liu, B.-Z.; Deng, H.-J.; Wu, G.-C.; Deng, K.; Chen, Y.-K.; Liao, P.; Qiu, J.-F.; Lin, Y.; Cai, X.-F.; et al. Antibody Responses to SARS-CoV-2 in Patients with COVID-19. *Nat. Med.* **2020**, *26*, 845−848.
(52) Long, Q.-X.; Tang, X.-J.; Shi, Q.-L.; Li, Q.; Deng, H.-J.; Yuan, J.; Hu, J.-L.; Xu, W.; Zhang, Y.; Lv, F.-J.; et al. Clinical and Immunological Assessment of Asymptomatic SARS-CoV-2 Infections. *Nat. Med.* **2020**, *26*, 1200−1204.
(53) Iyer, A. S.; Jones, F. K.; Nodoushani, A.; Kelly, M.; Becker, M.; Slater, D.; Mills, R.; Teng, E.; Kamruzzaman, M.; Garcia-Beltran, W. F.; et al. Persistence and Decay of Human Antibody Responses to the Receptor Binding Domain of SARS-CoV-2 Spike Protein in COVID-19 Patients. *Sci. Immunol.* **2020**, *5*, No. eabe0367.

https://doi.org/10.1021/acssensors.1c02215
ACS Sens. XXXX, XXX, XXX−XXX